

SPIN COATING IN SPIN-SPRAY LAYER BY LAYER SELF ASSEMBLY

MARRINER MERRILL

ABSTRACT. Spin-Spray Layer by Layer Self Assembly (SSLbL) is a new and promising method for ‘directed’ self assembly. SSLbL can be used to build materials that consist of tens to thousands of nanometer-thick layers rapidly and efficiently. These layers can be polymers, nanoparticles, or even biological colloids such as hemoglobin. One of the primary challenges to the development of SSLbL is a qualitative and quantitative understanding of spin coating thin films. This is because SSLbL works by sequentially spraying oppositely charged, dilute solutions directly onto a spinning disk. Optimization of cycle time, material waste, and resultant film quality are related to the mechanisms of spreading, evaporation, and charge-charge interaction that occur during the spin coating process. In this study, a qualitative understanding of spin coating is developed along with quantitative analysis of fundamental spin properties. These results are then used to indicate the important controlling variables in the spin environment experienced with SSLbL. In addition, an experimental setup is prepared to validate one hypothesis and initial results are given.

1. INTRODUCTION TO SSLBL

Spin-Spray Layer by Layer self assembly is a recent modification of Layer by Layer Self Assembly (LbL), which is a simple way of building up films in a layer by layer fashion using oppositely charged species [1]. LbL is very simple, and is carried out by dipping a substrate in a dilute solution of a negatively charged polymer (or colloid), then in a rinse, then in a dilute solution of a positively charged polymer (or colloid), and then in another rinse. At each step, the charge overcompensates, limiting film thickness and preparing the surface for the subsequent material. Each bilayer, also called a ‘cycle’ or a ‘nanolamina’ is on the order of one nanometer thick. Because there is no limit to the number of nanolaminae that can be stacked in a film, it is possible to build thin films with tens to hundreds of nanolaminae. Importantly, a given nanolamina does not depend strongly on the composition of previous layers, so it is possible to control the layered composition of a material on the order of a nanometer cheaply and simply.

Significant work has been done with LbL using different nanoparticles and polymers. Researchers have developed films using nanoclay [2, 3, 4], proteins [5, 6], carbon nanotubes [7], as well as many different polymers both to match given nanoparticles and for electrical, structural, or other properties [8]. Proposed uses for LbL created films range from batteries [9] to fuel cell membranes [10] to structural films [11, 12] to films for drug delivery or biomimetics [13].

Despite the simplicity of LbL, there are significant barriers to using it as a manufacturing method. Primarily, these are the slow rate of deposition, with LbL

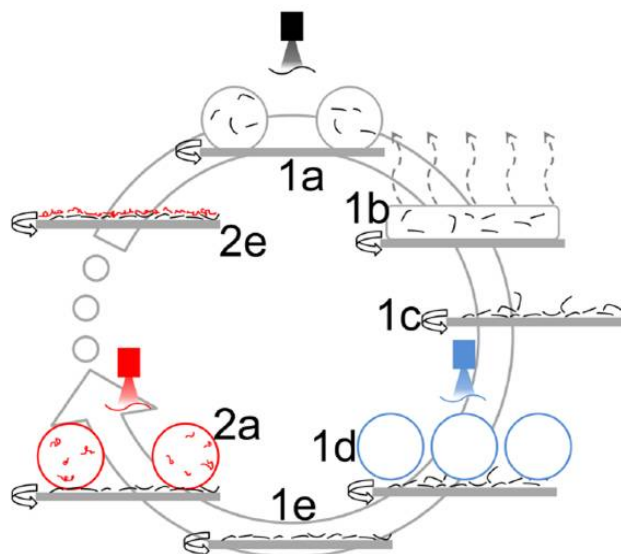


FIGURE 1. SSLbL Schematic. Step 1a-e shows the deposition of a negatively charged material (nanoclay), and step 2a-e shows the same cycle repeated for a positively charged polymer. [18]

cycle times generally on the order of 20 minutes or more, and the excessive waste of precursor materials. In a standard LbL film, less than 1% of the initial material is incorporated into the final film. The rest of the material is lost in the rinse stage or as a result of inevitable solution mixing as the substrate passes from one solution to another. Recently, a few variations of LbL have been developed to address the cycle time challenge: dewetting-LbL [14], spray LbL [15, 16], and spin-LbL [17, 11]. These methods have shown success in reducing cycle times to less than a minute, and also have resulted in some new possibilities for the final film structure and composition.

Spin-Spray LbL was developed to further increase cycle speed as well as to address the issue of material waste. Ideally, SSLbL uses spin coating to coat the surface with the precise right amount of a solution with no waste by spin-off. Evaporation of the solvent (water) leaves the polymers or particles attached to the surface. By using the same materials used in LbL, it is hypothesized that the fundamental attachment mechanisms could remain unchanged. Figure 1 shows a schematic of the process. SSLbL has proven to be successful to this point. Using simple spin coating assumptions, it has been possible to create nanoclay/polymer films hundreds of layers thick with good surface quality and material usage efficiency on the order of 50% [18].

To continue to improve the speed, quality, and efficiency of SSLbL, as well as to expand its use to other material systems, a better understanding of the spin coating process is necessary. Currently, most of the parameters in the SSLbL process (time before rinse, rinse volume, dry time) are chosen randomly or as a result of limited ad hoc testing. As SSLbL expands to new material systems, some quality problems arise, as can be seen in figure 2, where there are clearly problems with

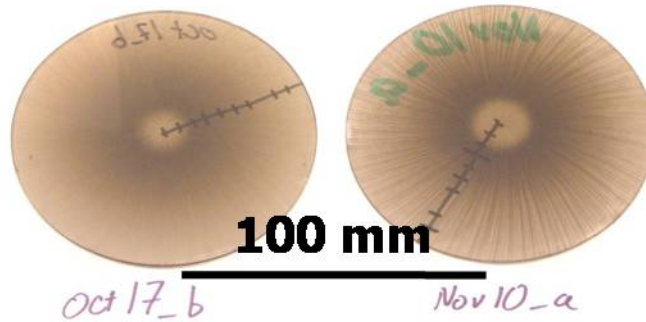


FIGURE 2. SSLbL results of two Carbon Nanotube films, one on a glass substrate, the other on polycarbonate. Note the radial streaks, indicating poor quality. Also, note that these streaks are more pronounced on the polycarbonate substrate.

coating uniformity in a Carbon Nanotube (CNT) film. The goal is to gain a better understanding of:

- (1) The amount of time that should be devoted to each step (spraying a solution, rinsing, drying, etc.).
- (2) The concentrations to use in the precursor solution
- (3) What parameters affect the quality of the completed film.

2. SPIN COATING

2.1. Infinite Spin coating. Spin coating has been a manufacturing process for many years, and there is a substantial body of literature regarding the process. Early fundamental fluids research was done by assuming an infinite plane, newtonian fluids, constant material properties in the thickness direction, and other so called ‘lubrication’ assumptions. One of the earliest papers examining spin coating in this way was written by Emslie, et. al in 1958 [19]. This work considered an infinite rotating fluid that was perfectly newtonian with the no slip boundary condition. In addition, gravity was neglected, though the radial momentum due to the spinning was not. By conservation of volume, Emslie developed a first order PDE for film thickness, h , and radius, r .

$$(1) \quad \frac{\partial h}{\partial t} = - \left(\frac{\rho \omega^2}{3\eta} \right) \frac{1}{r} \frac{\partial}{\partial r} (r^2 h^3)$$

where ρ is the density of the fluid, η is the dynamic viscosity, ω is the rotation rate, and t is time. Using a self-similar solutions, Emslie was able to show that even for initially very wavy films, the tendency was for the film to flatten quickly. Using the additional assumption of an initially flat film, it is possible to calculate the change in film thickness as:

$$(2) \quad \frac{dh}{dt} = - \frac{1}{r} \frac{d(qr)}{dt}$$

where q the volume flow rate, $\omega^2 r h^3 \rho / 3\eta$. Following this, the film thickness at any time is:

$$(3) \quad h = \frac{h_0}{\sqrt{1 + 4 \left(\frac{\rho \omega^2}{3\eta} \right) h_0^2 t}}$$

Equation 3 indicates a couple of important points. First is that there is no radial dependence. This is a fundamental benefit of spin coating, and a principle reason for its wide use, since films can be formed with very uniform thicknesses. Another important point is that the thickness reduces very rapidly in the initial stages. For example, a film initially 1 mm thick and a film initially 0.01 mm thick have only a 6% difference in thickness after 0.5 sec. Finally, the rate of thinning slows dramatically after this initial portion. For water, it would take on the order of a million seconds to get a film 2 nm thick.

The next stage in the development of spin physics is to add in the effects of evaporation. Meyerhofer [20] added this in by assuming that

- (1) Spin coating has two distinct regimes. The first is spin-off only (constant concentration), and the second is evaporation only (variable concentration, but no velocity in the radial direction).
- (2) The dividing line between these two regimes is when the rate of thinning by evaporation is equal to the rate of thinning by spin-off.
- (3) Evaporation is constant over all t and r .

These assumptions were primarily experimental, but they correctly predict the flow physics over a broad range of initial parameters. Meyerhofer predicted thinning of the form

$$(4) \quad \frac{dh}{dt} = -e \sim -\sqrt{\omega}$$

where e is a constant evaporation rate. The constant evaporation and its dependence on spin speed can also be seen in an earlier analytical work examining evaporation from a solid disk spinning in infinite space [21]. Later, the experimental constants that Meyerhofer used were connected to the properties of the solution and of the gas above the solution by Bornside [22], which gives the rate of thinning by evaporation as:

$$(5) \quad \frac{dh}{dt} = -\bar{k}\sqrt{\omega}(x_0 - x_\infty)$$

and the total thickness as a function of time:

$$(6) \quad h = \frac{h_0}{\sqrt{1 + 4 \left(\frac{\rho \omega^2}{3\eta} \right) h_0^2 t}} - \bar{k}\sqrt{\omega}(x_0 - x_\infty) t$$

where x is the concentration of solvent in the solution initially and in the final film at equilibrium. The \bar{k} constant in the problem was related to physical parameters as:

$$(7) \quad \bar{k} = \frac{c_g D_{sg}}{\rho_s \sqrt{v_g}} \frac{P_{sg} M_s}{RT}$$

where the subscripts indicate that the constants are properties either of the gas, the solution or both. The lack of subscripts above is because up to this point, all material constants referred only to the solution. Explanations for each material constant are listed, along with representative values for SSLbL in section 3, table 1.

Following this work, further research has been done by relaxing various assumptions. In many cases this has required numerical solutions. For example, the researchers above assumed that the properties of the solution were uniform in the thickness direction. Lawrence and others relaxed that assumption and found that the limiting parameter for film evaporation was most often not the development of a high concentration at the surface of the solution (a ‘skin’) but rather the diffusion of the solvent vapor through a saturated region right above the spinning disk[23, 24]. This provided further validation of Meyerhofer’s square root dependence for the evaporation. Further work has also been done to examine the development of striations, a common problem in photoresist coating. This has been primarily experimental, and it has been shown that possible marangoni and slight temperature changes might result in varying surface tension over the surface of the disk. Under the correct conditions, such variations lead to these radiating lines of thicker regions [25, 26, 27].

2.2. The Process. Another area of spin coating research has been in by assuming that the solution does not initially cover the substrate, but that it is spread over the substrate by the spinning. Analytical work has shown that this problem is identical to the downward flow of paint on a wall [28] or to the problem of a droplet spread by a jet impinging at the center [29]. The coating problem has also been extended to non-Newtonian liquids [30]. Although most of the analytical work is very approximate in nature and deals with more viscous, slower flows than are used in SSLbL, a few important qualitative results are still gleaned. One important one is an understanding of the conditions that lead to ‘fingering’ in spreading solutions. Fingering is when instead of the solution front moving uniformly, outwards, small regions of fluid will move far in advance of the main front. This would result in striations of the final films. It has been shown that fingering is driven almost entirely by surface-solvent interactions. And, for a high contact angle, fingers are developed that are long and tend to have straight sides [31].

2.3. Polymer/Particle Effects. Spin coating is usually carried out with polymers, and much of the early work was motivated by photoresist applications. However, as spin coating has become more mature, it has been used in a wider range of applications, including ultrathin films, low molecular weight polymers, nanoparticles, etc. At these extremes, behavior is often recognized that differs from that predicted above. Some of the characteristics which have been investigated are the minimum molecular weight at which entanglement occurs. It was found that this minimum is higher in spin coating[32] than in mixing, implying the need for a higher molecular weight polymer before entangling will occur. This has implications for the structural properties of spin coated films. Related work has been done by considering the mode of entanglement for polymers down to very low concentrations while being spun [33], including the suggestion to use spin coating to find a new polymer molecular weight. Finally, the dewetting stage of the process (during evaporation) has been studied[34]. Significantly, it does not appear that the spinning

had any effect on the dewetting characteristics other than that by spin coating, it is possible to form a thinner film of solution before dewetting begins than would be possible by other methods

Nanoparticles have also been considered. Two works that have relevance to SSLbL include another dewetting study and a hard-shell model. In the dewetting study, it was shown how particles can tend to agglomerate due to the receding meniscus ‘sucking’ smaller particles towards larger particles [35]. The hard-shell model was a numerical study examining spin coating of colloidal solutions. The interesting note is that for a presumed hard-shell particle interaction, the fluid behaved as a newtonian liquid [36].

2.4. Spin Coating and Electrostatics. Spin coating and LbL have been combined by other researchers as well, so some researchers have examined the effect of spin coating electrostatically charged polymers or particles. Some of these have been primarily focused on the development of unique structures, such as the development of perforated membranes by taking advantage of the dewetting behaviors described above [37]. Others have been more focused on fundamental work. Johal and others [38] experimentally built layered films using polymers with both opposite and like charges by spin coating. This was then compared with the same solutions in standard LbL. Since films can be built by spin coating from polymers that all contain the same charge, while this cannot be done with LbL, there are clearly additional factors at work, whether beneficial or not. Patel, et. al also combined spin coating with LbL for a range of different parameters. They found a radial thickness dependence for certain combinations of polymer charge strengths and solution concentration. They also examined the effect of increasing the salt concentrations of the polymer solutions [39].

3. QUANTITATIVE PARAMETERS

In order to begin to approach the ideal SSLbL case, it is important to be able to quantitatively define what parameters have an effect on final film thickness and quality. In the equations presented above, there are more than 10 different material properties that affect the spin coating process even with the assumption of a newtonian fluid. So, a parametric study was carried out to determine the effect of the various parameters. This study was done in two parts. In the first part, the baseline case was developed using the material constants that appeared to best approximate the current SSLbL setup. These parameters are listed in table 1. Note that the solution properties used are simply the properties of water. This is because the solute concentrations are so small (0.02%), that no effect on fluid flow is expected. The gas properties are those of dry air.

Then, each of these input parameters were considered to be independent and an uncertainty analysis was performed by varying each parameter 5% and examining the resultant change on the final properties. The final properties of interest were chosen as:

- (1) The time at which the spin-off step ends
- (2) The film thickness when the spin-off step ends
- (3) The time to totally dry the film
- (4) The thickness of the final film

TABLE 1. Baseline Material Constants for Typical SSLbL

Variable	Description	Value	Units
R	Universal Gas Constant	8.314	$\frac{J}{mol K}$
h_0	Initial film thickness	10	μm
ω	Disk rotation rate	314.2	$\frac{rad}{s}$
T	Temperature	293.15	K
ρ_s	Solution density	998.2	$\frac{kg}{m^3}$
η_s	Solution dynamic viscosity	0.001	$\frac{N \cdot s}{m^2}$
M_s	Solution molecular weight	0.018	$\frac{kg}{mol}$
x_0	Initial solvent concentration	0.9998	
x_∞	Equilibrium solvent concentration	0.10	
ν_g	Gas phase kinetic viscosity	1.48E-05	$\frac{m^2}{s}$
D_{sg}	Binary diffusivity of solvent vapor in gas	2.48E-05 [40]	$\frac{m^2}{s}$
P_{sg}	Vapor pressure of pure solvent in gas	2.34E+03	$\frac{N}{m^2}$
c_g	Evaporation constant	0.30 [21]	
Sc_g	Schmidt Number* ($\frac{\nu_g}{D_{sg}}$)	0.60	

*The Schmidt number is included because it is used to find the evaporation constant.

TABLE 2. Parametric Study

	Value	Total Uncertainty	Primary Variable	Secondary Variable
h1	2.0 μm	6.3%	Fluid Density (3.5%)	Rotation Rate (3.6%)
t1	1.0 sec	11%	Rotation Rate (5%)	Concentration (4%)
hf	0.40 nm	6.1%*	Concentration (20,000%)	Fluid Density (3.5%)
tf	3.0 sec	9.9%	Rotation Rate (5%)	Binary Diffusivity (3.4%)

*This neglects the contribution from the concentration

These properties are important because they indicate the SSLbL parameters to use. Total dry time indicates the time needed for drying, the thickness of the final film is an indicator of the solution concentration and volumes that should be used with each solution. The time until the solution is approximated to be ‘fixed’ to the surface indicates the amount of time available for individual droplets sprayed onto the surface to coalesce into a uniform film, if that is indeed possible.

The film thicknesses were found following the work of Meyerhofer, basically when equations 2 and 5 are equal. The thickness of the final film was done by continuing with the assumption of no spin-off, and calculating the final thickness assuming that all solvent evaporated leaving a uniform film of polymers with a specific gravity of 1.0. Since the equations given generally solve explicitly for thickness, the time to that thickness is solved using a matlab function.

After running the uncertainty analysis, the results are summarized in table 2. Here the total uncertainty is found using the sum of the squares of the uncertainty from each (presumed independent) variable. The next two columns indicate which the two material parameters that had the greatest effect on the result, along with the percent uncertainty in the final result caused by the one variable.

TABLE 3. Study of Rotation Rate and Temperature (% change is shown)

	Value	Rotation = 5000 rpm	Ts = 10 C	Tg = 10 C	Tall = 10 C
h1	2.0 μm	23%	9.3%	19%	11%
t1	1.0 sec	39%	8.4%	55%	69%
hf	0.40 nm	23%	9.3%	19%	11%
tf	3.0 sec	30%	9.3%	53%	67%

The primary outcomes of Table 1 are that the final properties are actually fairly stable to variation from the initial parameters. With the other uncertainties involved, 10% is not bad. The other important point is that a few parameters come up as the most important: the rotation rate, the concentration, the density and the binary diffusivity (the diffusivity of water vapor in air). The very large contribution by concentration to final film thickness is expected, since an increase in solute concentration from 0.02% to 5.02% results in a much thicker film. Note, however, that this did not significantly impact any other results.

The second part of the quantitative study was done by recognizing that temperature and rotation rate are the two parameters that change the most. Also, in the case of temperature, a change in temperature results in a change in many other parameters as well, such as viscosity. Such dependencies were neglected in the uncertainty analysis.

Three different cases were considered and compared to the baseline. First, the rotation rate was changed from 3,000 rpm to 5,000 rpm. Next, the temperature of the substrate (and by the thin film approximation, the solution) was decreased by 10°C, then the effect of decreasing the gas temperature by 10°C. And finally, the effect of decreasing both solution and gas temperature. The results are summarized in table 3.

As expected, the variation was much more significant. It is important to note, though, that even a dramatic change in substrate temperature does not change total nearly as much as a change in the temperature of the gas above the substrate. This is an important note for SSLbL, since the constant nature of the SSLbL process results in the gradual cooling of the substrate, which is difficult to avoid. At the same time, small deviations in the air temperature will have a much more dramatic effect.

4. EXPERIMENTAL WORK

One of the primary flaws in current films is the development of radial striations. From the literature review above, striations appear to be caused either during the drying stage of uniform films [26] or as a result of fingering during solution spreading [31]. Because of the difference noted for the glass and polycarbonate substrates in figure 2, it is hypothesized that the spreading is more likely the problem. Since this is a function of the dewetting between the CNT solution and its counter-solution, there is value in examining this effect. An experiment has been designed to do so.

4.1. Experimental Setup. Actual substrate effects are easy to control by surface treatments before film deposition begins. However, even on the ‘good’ substrate, the striations occur, so it is assumed that the contact angle between the CNT solution and the existing film could be a driver. The contact angle of the existing

film is primarily a function of the counter solution used with the CNT solution. So, several different polymers (with different wetting characteristics) are used for the counter solution:

- Poly(vinyl alcohol) - neutral
- Poly(diallyldimethylammonium chloride) - positive
- Poly(ethylene imine) - slightly positive
- Poly(ethylene imine) - slightly positive, high concentration
- Poly(acrylic acid) - negative

These five different polymers are all standard materials for LbL films. The CNT solution is a solution of Multi-Walled CNT's that have been 'wrapped' in a slightly negatively charged polymer. The experimental plan is to create films from each of these and examine

Initial and final contact angles: of the CNT solution on the substrate or film. Initial contact angle is found by starting deposition with the counter polymer solution and then measuring the contact angle. Then, after 50 cycles of CNT-polymer (ending with the counter polymer), measuring the contact angle again. Together, these angles will indicate the amount of dewetting initially and the 'steady-state' contact angle, since it is assumed that by 50 cycles steady state growth has been reached.

Electrical Conductivity: of the film after 50 cycles. This gives an indirect measure of the amount of CNT that was incorporated into the film.

Visual Inspection: for the existence and magnitude of striations including the radial location at which they appear to have begun. Of course, the counter solution also effects the amount of CNT that is deposited, and therefore how dark the film is. In order to compare two films, the photographs will be manipulated so that the underlying tint is fairly close, in this way, thicker, more definite striations in one film will indicate a greater effect.

For the SSLbL process and electrical conductivity measurements, existing equipment could be used. However, a method of measuring water contact angle had to be incorporated into the existing spin-spray setup. This was done using a microscope camera, a low magnification microscope and a halogen lantern. The setup is shown in figure 3. Then in figure 4 a picture of a representative droplet is shown. The basic procedure used is to put a drop of liquid on the substrate and immediately take a picture, then if possible, expand the drop with some more fluid and take another picture. The contact angles are measured and the average is taken. To validate the setup, measurements were made for the contact angle of distilled water on polycarbonate. The result was $93^\circ \pm 4^\circ$. Values reported in the literature ranged from 72° to 93° [41, 42]. Because contact angle is a function of the type of polycarbonate and its surface treatment, it was assumed that the variability seen results from this, and that the measured value indicates that the experimental setup is working.

4.2. Preliminary Results. Although the entire series of tests have not yet been run, preliminary results have been achieved for the two concentrations of poly(ethylene imine). Basic results are shown in table 4 and figure 5. At this stage, the important 'conclusions' are simply that the experimental setup is working, there is a difference



FIGURE 3. Photograph of the experimental setup for measuring contact angle in situ. This consists of a camera and microscope, with the substrate mounted on the SSLbL robot, illuminated from behind with a light.

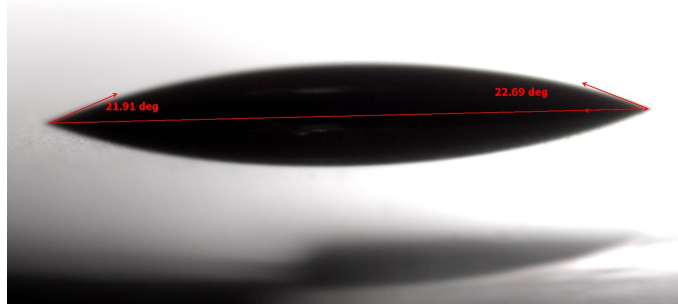


FIGURE 4. The picture of a droplet is shown immediately after deposition. Contact angle measurement is done by measuring the contact angle on either side of the droplet (as drawn) and averaging.

TABLE 4. Preliminary Results

Test	Initial Angle (deg)	Final Angle (deg)	Final Resistivity (Ohms)
dec13a - 0.02% PEI	8.6	30.4	10^9
dec13b - 0.14% PEI	10	22.5	10^7

in contact angle, and there is a difference in the degree of striation from one film to the next.

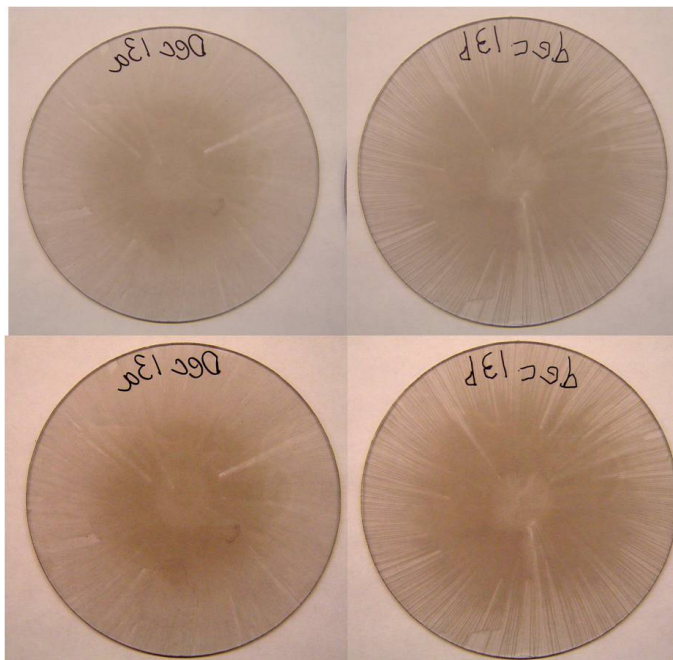


FIGURE 5. Preliminary results for contact angle study. Note that the two pictures on top are the original and the two on the bottom have been modified so that the color at the center of the disk matches, allowing for more direct comparison.

5. CONCLUSIONS

The primary conclusions of this study are that SSLbL is a valuable method, but in order to improve it, a better understanding of spin coating is required. Through a literature survey, a parametric study, and some experimental work, the governing parameters are being defined (spin speed, temperature of gas), and keys to improving the SSLbL process are identified. These include time to dry a film, deposition time, as well as some initial indicators of the importance of the water contact angle.

REFERENCES

- [1] Decher G 1997 *Science* **277** 1232–1237
- [2] Mamedov A, Ostrander J, Aliev F and Kotov N A 2000 *Langmuir* **16** 3941–3949
- [3] Podsiadlo P, Kaushik A, Arruda E, Waas A, Shim B S, Xu J, Nandivada H, Pumplin B, Lahann J, Ramamoorthy A and Kotov N 2007/10/05 *Science* **318** 80 – 83
- [4] Podsiadlo P, Paternel S, Rouillard J M, Zhang Z F, Lee J, Lee J W, Gulari L and Kotov N A 2005 *Langmuir* **21** 11915–11921
- [5] Zhou Y, Li Z, Hu N, Zeng Y and Rusling J F 2002 *Langmuir* **18** 8573–8579
- [6] Mehta G, Kiel M J, Lee J W, Kotov N, Linderman J J and Takayama S 2007 *Adv. Funct. Mater.* **17** 2701–2709
- [7] Mamedov A A, Kotov N A, Prato M, Guldi D M, Wicksted J P and Hirsch A 2002 *Nat. Mater.* **1** 190–194
- [8] Lutkenhaus J L and Hammond P T 2007 *Soft Matter* **3** 804–816
- [9] Cassagneau T and Fendler J H 1998 *Advanced Materials* **10** 877–+

- [10] Michel M, Taylor A, Sekol R, Podsiadlo P, Ho P, Kotov N and Thompson L 2007 *Advanced Materials* **19** 3859 – 3864
- [11] Jiang C, Markutsya S and Tsukruk V V 2004 *Advanced Materials* **16** 157–161
- [12] Tang Z Y, Kotov N A, Magonov S and Ozturk B 2003 *Nat. Mater.* **2** 413–U8
- [13] Jiang C Y and Tsukruk V V 2006 *Advanced Materials* **18** 829–840
- [14] Shim B S, Podsiadlo P, Lilly D G, Agarwal A, Lee J, Tang Z, Ho S, Ingle P, Paterson D, Lu W and Kotov N A 2007 *Nano Lett.* **7** 3266 – 3273
- [15] Krogman K, Zacharia N, Schroeder S and Hammond P 2007 *Langmuir* **23** 3137 – 3141
- [16] Schlenoff J B, Dubas S T and Farhat T 2000 *Langmuir* **16** 9968 – 9969
- [17] Cho J, Char K, Hong J D and Lee K B 2001 *Advanced Materials* **13** 1076–+
- [18] Merrill M and Sun C in press *Nanotechnology*
- [19] Emslie A G, Bonner F T and Peck L G 1958 *J. Appl. Phys.* **29** 858–862
- [20] Meyerhofer D 1978/07/ *Journal of Applied Physics* **49** 3993 – 7
- [21] Kreith F, Taylor J H and Chong J P 1959 *ASME. J. of Heat Transfer* **81** 95–105
- [22] Bornside D, Macosko C and Scriven L 1991 *J. Electrochem. Soc.* **138** 317 – 320
- [23] Lawrence C 1990/03/ *Physics of Fluids A (Fluid Dynamics)* **2** 453 – 6
- [24] Ohara T, Matsumoto Y and Ohashi H 1989/12/ *Physics of Fluids A (Fluid Dynamics)* **1** 1949 – 59
- [25] Birnie DP I and Manley M 1997/04/ *Physics of Fluids* **9** 870 – 5
- [26] Birnie DP I 2001/04/ *J. Mater. Res.* **16** 1145 – 54
- [27] Haas D E, Quijada J N, Picone S J and Birnie D P I 2000 vol 3943 (Bellingham, WA, USA) pp 280 – 284
- [28] Schwartz L and Roy R 2004 *Physics of Fluids* **16**
- [29] McKinley I and Wilson S 2002 *Physics of Fluids* **14** 133 – 142
- [30] Charpin J, Lombe M and Myers T 2007/07/ *Physical Review E (Statistical, Nonlinear, and Soft Matter Physics)* **76** 16312 – 1
- [31] Eres M, Schwartz L and Roy R 2000 *Physics of Fluids* **12** 1278 – 1295
- [32] Bernazzani P, Simon S, Plazek D and Ngai K 2002/05/ *European Physical Journal E* **8** 201 – 7
- [33] Schubert D W and Dunkel T 2003 *Materials Research Innovations* **7** 314 – 321
- [34] Muller-Buschbaum P, Hermsdorf N, Gutmann J, Stamm M, Cunis S, Gehrke R and Petry W 2004// vol B43 (USA) pp 29 – 42
- [35] Phadke S, Stanley J R, Sorge J D and Birnie III D P 2007 *Journal of the Society for Information Display* **15** 1089 – 1093
- [36] Rehg Timothy J and Higgins Brian G 1992 *AIChE J.* **38** 489 – 501
- [37] Zimmitsky D, Shevchenko V V and Tsukruk V V 2008 *Langmuir* **24** 5996 – 6006
- [38] Johal M S, Casson J L, Chiarelli P A, Liu D G, Shaw J A, Robinson J M and Wang H L 2003 *Langmuir* **19** 8876 – 8881
- [39] Patel P A, Dobrynin A V and Mather P T 2007 *Langmuir* **23** 12589 – 12597
- [40] Massman W 1998 *Atmospheric Environment* **32** 1111 – 1127
- [41] Gil'man A, Drachev A, Vengerskaya L, Semenova G, Kuznetsov A and Potapov V 2003 *High Energy Chemistry* **37** 267–271
- [42] Sharma R, Holcomb E, Trigwell S and Mazumder M 2007 *Journal of Electrostatics* **65** 269 – 273